Available at: http://publications.ictp.it IC/2010/036

United Nations Educational, Scientific and Cultural Organization
and
International Atomic Energy Agency

THE ABDUS SALAM INTERNATIONAL CENTRE FOR THEORETICAL PHYSICS

EMPIRICAL MODEL FOR ELECTRON IMPACT IONIZATION OF HYDROGEN ISOELECTRONIC IONS

A.K.F. Haque[1]
Department of Physics, University of Rajshahi, Rajshahi-6205, Bangladesh
and
The Abdus Salam International Centre for Theoretical Physics, Trieste, Italy,

M.R. Talukder
Department of Applied Physics and Electronic Engineering, University of Rajshahi, Rajshahi-6205, Bangladesh,

M.A. Uddin, M. Shahjahan, A.K. Basak
Department of Physics, University of Rajshahi, Rajshahi-6205, Bangladesh

and

B.C. Saha
Department of Physics, Florida A & M University, Tallahassee, Florida 32307, USA.

MIRAMARE – TRIESTE

June 2010

[1] Associate of ICTP. Corresponding author: ahaque@ictp.it; fhaque2001@yahoo.com

Abstract

The total cross sections of electron impact single ionization, for hydrogen like H, He^{+}, Li^{2+}, B^{4+}, C^{5+}, N^{6+}, O^{7+}, Ne^{9+}, Ar^{+17}, Fe^{25+}, Mo^{41+}, Dy^{65+}, Au^{78+}, Bi^{82+}, and U^{91+} targets with incident electron energies from threshold to about $10^{6}\ eV$, are calculated using a modified version of the BELI model [Bell *et al.*, J. Phys. Chem. Ref. Data 12, 891 (1983)] by incorporating ionic correction factor in it and expressing its parameters in terms of the ionization potential of the ionized orbit. The results of the present analysis are compared with the available experimental results and theoretical calculations. The proposed model calculates reasonably accurate cross sections for any hydrogen isoelectronic ions with atomic numbers in the range of Z = 1-92. The level of performance of the simple model is at least comparable with other existing methods and models.

1. Introduction

Electron impact ionization (EII) cross sections are widely used in applied fields [1] such as modeling of fusion plasmas, modeling of radiation effects for both medical and materials research, aeronomy, and fundamental research in atomic, molecular, and astrophysics. Many quantum mechanical models have been proposed [2-8] for atoms and ions to calculate electron impact single ionization (EISI) cross sections. These methods solve the Schrödinger equation and are capable of deducing differential ionization cross-sections as well as the total ionization cross sections. In particular, quantum methods such as the R-matrix method, distorted wave Born approximation (DWBA) and convergent close coupling method have, using a variety of numerical methods, been employed to calculate cross sections. However, quantum methods with approximation in applications provide cross sections for discrete energies and selected species. On the other hand, experiments are difficult to implement and costly as well. Besides, the quantum methods require large computational resources and computational time. Moreover, quantum procedures do not usually provide the user with speedy and forthwith calculations, as required by the practitioners in the field of applied sciences. The requirement can be best fulfilled by analytic models, which can provide fast generation of reliable cross sections over the wide domains of validity. Hence, this necessitates a simple-to-use model that can calculate EISI cross sections for scientific and industrial applications.

Many empirical, semi-empirical, classical, and semi-classical models are reviewed and proposed [9 - 25]. Deutsch-Mark (DM) [10], Lotz [15,16], Bell *et al.* (BELI) [17] models, and the binary-encounter-dipole (BED) model [19] have been extensively used to calculate cross sections. The DM and BED models have been used for calculating cross sections of molecules and atoms. The MRIBED (modified relativistic BED) [20] model calculates EISI cross sections for selected species. A number of empirical models have been propounded [17] for calculating cross sections without generalization of model parameters. Simple empirical models, proposed in [23, 24], are valid either for very much selected targets or, in many cases, applicable to low incident energies. However, a user-friendly model capable of calculating sufficiently accurate EISI cross sections for a wide variety of species and range of energies may contribute to fill up, to some extent, the gap between the available cross sections data and the demand level.

The empirical BELI model [17] has been used to fit data for light atomic targets using species-dependent values of the parameters of the model. Haque *et al*. proposed the MBELL model [26 - 29], modifying the BELI model by incorporating ionic and relativistic corrections, and applied with success to the computation of *K*-shell [26], *L*-shell [27, 28] and *M*-shell [29] EISI cross sections for a wide domain of atoms. In the above applications, the parameters of the MBELL model are generalized in terms of the ionized orbital's, but are not expressed in terms of any orbital property. Talukder et al. [25] expressed the parameters of the

BELI model in terms of the ionization potential I_{nl} of the ionized orbits with quantum numbers (nl) and achieved with reasonable success in accounting for the ionization cross sections for the open and closed shell neutral atoms in the wide range of $1 \leq Z \leq 92$ for energies up to about 10 keV. It might be of interest to investigate the dependence of the generalized parameters of the MBELL model on I_{nl} of the ionized orbit concerned.

With this motivation, this work proposes a simple model incorporating an ionic correction factor like the one infused in the MBELL model [26 - 29] and making the parameters dependent on the ionization potential to reduce the number of fitting parameters and improve the efficacy of the model. The model so framed is, henceforth, referred to as the MSBELL model.

We apply the proposed MSBELL model to calculate the EISI cross sections of H, He^{+}, Li^{2+}, B^{4+}, C^{5+}, N^{6+}, O^{7+}, Ne^{9+}, Ar^{+17}, Fe^{25+}, Mo^{41+}, Dy^{65+}, Au^{78+}, Bi^{82+}, and U^{91+} from the hydrogen-isoelectronic sequence. The prediction from the MSBELL model is compared with the available experimental results and other theoretical calculations.

This paper is organized as follows. The MSBELL model is sketched in Section 2. In Section 3, we discuss the results of MSBELL in comparison with the experimental results and other theoretical calculations. Section 4 is devoted to the discussion of the results and the conclusions arrived at.

2. Outline of the model

The semi-empirical BELI formula [17] for the EISI cross sections of atoms and ions, originating from the work of Bell *et al.* [18], is of the form

$$\sigma_{BELI}(E) = \frac{1}{EI}\left\{ A\ln(E/I) + \sum_{k=1} B_k (1 - I/E)^k \right\}. \qquad (1)$$

Here, E is the kinetic energy of the incident electron, I is the ionization potential; A and B_k's are the fitting coefficients.

We propose an empirical model to improve the efficiency and to reduce the number of fitting coefficients of the BELI model [18] for the description of EISI cross sections to cover the wide range of ionic targets from $Z = 1 - 92$. In the simplified form of Eq. (1), σ_{SBELL} is given by

$$\sigma_{SBELL}(E) = \sum_{nl} \frac{N_{nl} I_{nl}}{E} \left\{ A_{nl} \ln(E/I_{nl}) + B_{nl}(1 - I_{nl}/E) \right\}, \qquad (2)$$

where A_{nl} and B_{nl} are the fitting parameters expressed as the function of normalized potential $U_R = I_{nl}/R$ with R as the Rydberg energy. E is the incident energy. E and I_{nl} are both expressed in eV. N_{nl} is the number of electrons in the ionizing nl orbit. The first term with the parameter A_{nl} represents the Bethe formula determining the high energy behavior of the cross section. Here the summation is over the orbit nl of the target. It is noted that one

can neglect the summation symbol for hydrogen isoelectronic sequence because the targets have only 1*s* orbital in Eq. (2), thereby leading to only two orbital dependent parameters A_{nl} and B_{nl} in the case of the hydrogen-like atoms. This formula also ensures the correct behavior of the cross sections at both low and high impact energies. However, Eq. (2) is modified by incorporating in it the ionic correction factor to extend the applicability of BELI model for ionic targets. It has been noted that the ionic effect decreases with the increase of the incident electron energy [30]. In light of this fact, we suggest an ionic correction [30] in the form of a multiplying factor F_I

$$F_I = 1 + n\left(\frac{q}{ZU_R}\right)^{\lambda}, \qquad (3)$$

where n and λ are fitting parameters. The optimum values obtained for n and λ, as discussed later, are $n = 1.5$ and $\lambda = 0.5$.

Finally, Eqs. (2) and (3) lead to the expression for the EISI cross section, σ_{MSBELL}, in the proposed MSBELL model given by

$$\sigma_{MSBELL} = F_I \sigma_{SBELL}(E). \qquad (4)$$

In Eq. (4), the fitting parameters A_{nl} and B_{nl} are generalized by making them dependent on I_{nl}. The parameters A_{nl} and B_{nl} are expressed as

(a) for $1 \le U_R \le 100$

$$A_{nl} = \frac{1.44\times10^{-10}U_R}{(1+69U_R)^{3.08}}, \qquad (5a)$$

$$B_{nl} = -\frac{1.72\times10^{-10}U_R}{(1+69U_R)^{3.15}}, \qquad (5b)$$

(b) $100 \le U_R \le 10^4$

$$A_{nl} = \frac{2.38\times10^{-11}U_R}{(1+69U_R)^{2.90}}, \qquad (5c)$$

$$B_{nl} = -\frac{2.11\times10^{-11}U_R}{(1+69U_R)^{2.94}}, \qquad (5d)$$

Ionization potential is normalized by $U_R = I_{nl}/R$, where R is the Rydberg energy. The units of A_{nl} and B_{nl} are expressed in cm^2.

3. Results and discussions

We have used the published results for ionization potentials of neutral targets given by Desclaux [31]. On the other hand, the ionization potentials for the ionic targets are calculated using the Dirac-Hartree-Fock code [32]. Using the MSBELL model we have calculated EISI cross-sections for the hydrogen isoelectronic sequence, using Eq. (4) along with Eqs. (5), over a wide incident electron energies from threshold to 10^6 *eV*. The results presented here only

for H, He^{+}, Li^{2+}, B^{4+}, C^{5+}, N^{6+}, O^{7+}, Ne^{9+}, Ar^{+17}, Fe^{25+}, Mo^{41+}, Dy^{65+}, Au^{78+}, Bi^{82+}, and U^{91+} targets for which experimental or theoretical results are available. Most recent experimental as well as theoretical results are taken into account to compare the results obtained by the MSBELL model. It is interesting to note that this model can be used for the description of EISI cross sections for any hydrogen-like target from H to U.

The ionic correction factor F_I in Eq. (3) with the parameter values $n = 1.5$ and $\lambda = 0.5$ are optimized in such a way that Eq. (4) describes the best EISI cross sections with respect to the experimental data for the range of incident energies and for the targets considered herein. The coefficients of the parameters A_{nl} and B_{nl} in Eqs. (5a) – (5d) are determined from the overall best fits of our predicted cross sections to the experimental results. A measure of the quality of best fit is obtained by minimizing the chi-square defined by

$$\chi^2 = \sum_i \left[\frac{\sigma_c(E_i) - \sigma_x(E_i)}{\sigma_x(E_i)} \right]^2 ,$$

where $\sigma_c(E_i)$ and $\sigma_x(E_i)$ refer, respectively, to the theoretical and experimental cross sections at the energy point E_i. The optimum values of the coefficients, in terms of which the parameters A_{nl} and B_{nl} are defined, are obtained using a non-linear least-square fitting program.

In the figures, open- and filled symbols represent, respectively, the quantum and experimental results. On the other hand, the thick continuous line represents the prediction by the proposed model while the dashed lines are the predictions by classical, semi-classical, or empirical formula.

Figures 1(a-c) show the EISI cross sections of H, He^{+}, and Li^{2+}, respectively. The MSBELL predictions for H are displayed in Fig. 1(a), along with the experimental cross sections [33] and the results of TPDW01 (relativistic two-potential distorted-wave approximation [34]), MRIBED [35], and DM [10] theories. The TPDW01 and DM results significantly overestimate the experimental results over the almost entire range of incident energies. The MSBELL and MRIBED calculations are almost identical and agree well with the experimental findings. In Fig. 1(b), we present the calculated cross sections for He^{+}, experimental results [36], and findings from the TPDW01 [34], DM [10], and MRIBED [35] theories. A small discrepancy is found with MSBELL calculations and the experimental results in the peak region but the MSBELL and TPDW01 results agree well. MSBELL predictions for Li^{2+} are depicted, in Fig. 1(c), along with the experimental cross sections [37] and the FRDWBA (fully relativistic DWBA [38]), MRIBED [35], DM [10], and DWBA [39] results. The MRIBED calculations slightly underestimate in the range 200-600 eV while FRDWBA results overestimate the experimental results beyond 3 keV. Theoretical results of DM, DWBA, MRIBED, and MSBELL are almost identical. However, comparisons among the experimental and theoretical findings demonstrate that the MSBELL results are the best.

Figures 2 (a-c) display the EISI cross sections of B^{4+}, C^{5+} and N^{6+}, respectively. The MSBELL predictions for B^{4+} are displayed, in Fig. 2(a), along with the experimental results [40], and the theoretical FRDWBA [38], DWBA [39], and MRIBED [35] findings. The predictions from the MSBELL model for the three targets are completely identical, and excellent agreements are found with the experimental results over the wide incident energies. The MSBELL model definitely performs better than either of FRDWBA, DWBA, and MRIBED models. In Fig. 2(b), we present the calculated cross sections for C^{5+}, experimental results [40, 41], and theoretical findings from DWBA [39], TPDW01 [34], and MRIBED [35]. All theoretical calculations, except that of MRIBED from peak to high incident energies, are identical with the experimental results. Among all the theories, the best agreement is found between the experimental [40] and MSBELL results over the wide incident energies. The MSBELL predictions for N^{6+} are depicted, in Fig. 2(c), along with the experimental cross sections [40, 41] and the theoretical FRDWBA [38], DWBA [39], MRIBED [35], and DM [10] findings. In this case also, the MSBELL predictions agree excellently with the experimental results [40] over the entire domain of incident energies. The MSBELL predictions are completely successful for the description of EISI cross sections for B^{4+}, C^{5+} and N^{6+} targets over incident energies considered herein than the theoretical findings of FRDWBA, DWBA, TPDW01 and MRIBED.

In Figs. 3(a-c), we compare the MSBELL predictions for the EISI cross sections of O^{7+}, Ne^{9+}, and Ar^{17+} targets, respectively, with the experimental cross sections [40, 41]. The other theoretical calculations used for comparison in these figures are DWBA [39], FRDWBA [38], MRIBED [35], of Kunc [42], and DWBE (distorted-wave Born exchange [43]). The MSBELL and DWBA results agree well with the experimental measurements, as seen in Fig. 3(a) for O^{7+}. The DM and MRIBED calculations slightly underestimate the experimental results in the low energy region while slightly overestimate from peak to high energy region. The prediction of MSBELL is the better than that of DM and MRIBED calculations. In Fig. 3(b), both the MSBELL and DM calculations underestimate the experimental results in the peak region. But the MSBELL results are better than those of DM. However, in case of Ar^{17+}, as shown in Fig. 3(c), MSBELL produces excellent agreement with the experimental results as well as with the DWBE calculations. The new MSBELL model comes out as the best performer in reproducing the experimental cross sections for O^{7+}, Ne^{9+}, and Ar^{17+} targets over incident energies considered herein.

Figures 4(a-c) illustrate the EISI cross sections of Fe^{25+}, Mo^{41+}, and Dy^{65+}, respectively. The MSBELL calculations for Fe^{25+} are displayed in Fig. 4(a), along with the experimental cross sections [44] and the results of FRDWBA [38], and O'Rourke [45] theories. The MSBELL and FRDWBA calculations are identical and fairly good agreements of MSBELL predictions with the experimental results are found within the experimental error. In Fig. 4(b), we present the calculated MSBELL cross sections of Mo^{41+}, experimental results [44, 46], and

theoretical findings from the DWBA [39], and FRDWBA [38]. The DWBA and MSBELL calculations are identical in pattern, but the DWBA calculations slightly underestimate the experimental results while a better agreement is found for the MSBELL results within the experimental error. The MSBELL predictions of Dy^{65+} are depicted, in Fig. 4(c), along with the experimental cross sections [42] and the theoretical FRDWBA [38], DWBA [39], RDWBA [47] and MRIBED [35] findings. Fairly good agreement is found between the MSBELL predictions and the experimental results [44]. As a whole, the MSBELL predictions are successful for the description of EISI cross sections for Fe^{25+}, Mo^{41+}, and Dy^{65+} targets over the incident energies considered herein than the theoretical findings of FRDWBA, DWBA, RDWBA, and MRIBED.

Figures 5(a-c) display the MSBELL calculations for Au^{78+}, Bi^{82+}, and U^{91+}. In Fig. 5(a), we compare the experimental EISI cross sections [48], along with the findings of FRDWBA [38], and RDWBA [47] theories. The MSBELL calculations slightly overestimate the experimental results, but the pattern is identical with respect to the FRDWBA, and RDWBA calculations. The MSBELL predictions are, depicted in Fig. 5(b) for Bi^{82+}, compared with the experimental findings [48], along with the results of DWBA [39], and MRIBED [35] theories. The DWBA calculations slightly underestimate the experimental measurements over the incident energies considered herein. The MRIBED results increase with the increase of incident energy due to the inclusion of relativistic effect in their model. An identical pattern is observed between the DWBA and MSBELL results over the domain of incident energies. However, an excellent agreement is found between the MSBELL calculations and the experimental results. Fig.5(c) compares the MSBELL findings with the experimental results [48] together with the TPDW01 [34], RDWBA [47], DWBA [39], and FRDWBA [38] calculations, for U^{91+}. Calculations of TPDW01, RDWBA, and FRDWBA theories underestimate the experimental results over the wide incident energies. The MSBELL results agree well with the experimental finding and the DWBA calculations. Cross sections, calculated by the MRIBED and DWBA theories, increase with the increase of incident energy due to the influence of relativistic effect. Finally, the MSBELL calcculate successfully, with respect to the other theoretical results considered herein, describe the EISI cross sections for Au^{78+}, Bi^{82+}, and U^{91+} targets over the domain of incident energies.

4. Conclusions

The MSBELL model is seen to provide a good description of the experimental EISI cross section data for any hydrogen like targets with the atomic number $Z = 1 - 92$ and with the incident electron energies from threshold to $10^6\ eV$. In the description of the available experimental data with respect to the domain of species and incident energies, the level of performance of the present model seems to be the best or as good as the other sophisticated theoretical methods, like DWBA, TPDW01, FRDWBA, considered herein for comparison. It

is demonstrated that the present MSBELL model provides very encouraging and reliable results for the EISI cross sections. In order to decide the predictive role of our model, it is our intention to extend this model to other isoelectronic systems. However, the MSBELL model with its simple structure may turn out to be an efficient method for the calculations of EISI cross sections for hydrogen like targets for applications.

Acknowledgments

This work was done within the framework of the Associateship Scheme of the Abdus Salam International Centre for Theoretical Physics (ICTP), Trieste, Italy. One of us (A. K. F. Haque) would like to thank ICTP for kind hospitality and support.

References

1. Talukder, M.R.; Korzec, D.; Kando, M. J. Appl. Phys. 2002, **91**, 9529.
2. Baertschy, M; Rescigno, T.N.; McCurdy, C.W. Phys. Rev. A 2001, **64**, 022709.
3. S. Jones, D.H.; Madison, Phys. Rev. A 2000, **62**, 042701.
4. Fursa, D.V.; Bray, I. Phys. Rev. A 1995, **52**, 1279.
5. Kato, D.; Watanabe, S. Phys. Rev. Lett. 1995, **74**, 2443.
6. Chang, J.C.; Sun, H.L.; Cheng, W.Y.; Huang, K.N. Phys. Rev. A 2004, **69**, 052713.
7. Bray, I. J. Phys. B 1995, **28**, L247.
8. Bray, I. Phys. Rev. A 1992, **46**, 6995.
9. Younger, S. M.; Märk, T. D. in: T.D. Mark G.H. Dunn (Eds.), Electron Impact Ionization, Springer-Verlag, Berlin, 1985, p. 24.
10. Deutsch, H.; Märk, T.D. Int. J. Mass Spect. Ion Proc. 1987, **79**, R1.
11. Deutsch, H.; Becker, K.; Matt, S.; Märk, T.D. Int. J. Mass Spect. 2000, **197**, 37.
12. Margreiter, D.; Deutsch, H.; Märk, T.D. Int. J. Mass Spect. Ion Proc. 1994, **139**, 127.
13. Deutsch, H.; Becker, K.; Matt, S.; Märk, T.D. Contrib. Plasma Phys. 1995, **35**, 421.
14. Deutsch, H.; Becker, K.; Gstir, B.; Märk, T.D. Int. J. Mass Spect. 2002, **213**, 5.
15. Lotz, W. Z. Phys. 1968, **216**, 241.
16. Lotz, W. Z. Phys. 1970, **232**, 101.
17. Godunov, A.L.; Ivanov, P.B. Phys. Scr. 1999, **59**, 277.
18. Bell, K.L.; Gilbody, H.B.; Hughes, J.G.; Kingston, A.E.; Smith, F.J. J. Phys. Chem. Ref. Data 1983, **12**, 891.
19. Kim, Y.-K.; Rudd, M.E. Phys. Rev. A 1994, **50**, 3954.
20. Uddin, M.A.; Haque, A.K.F.; Basak, A.K.; Karim, K.R.; Saha, B.C. Phys. Rev. A 2005, **72**, 032715.
21. Talukder, M.R.; Bose, S.; Takamura, S. Int. J. Mass Spectrom. 2008, **269**, 118.
22. Gryzinski, M. S. Phys. Rev. 1965, **138**, 336.
23. Bernshtam, V. A.; Ralchenco, Y. V.; Maron, Y. J. Phys. B 2000, **33**, 5025.

24. Kim, Y.K.; Desclaux, J.P. Phys. Rev. A 2002, **66**, 012708.
25. Talukder, M.R.; Bose, S.; Patoary, M.A.R.; Haque, A.K.F.; Uddin, M.A.; Basak, A.K.; Kando, M. Eur. Phys. J. D 2008, **46**, 281.
26. Haque, A.K.F.; Uddin, M.A.; Basak, A.K.; Karim, K.R. and Saha, B.C. Phys. Rev. A 2006, **73**, 0122708.
27. Haque, A.K.F.; Uddin, M.A.; Basak, A.K.; Karim, K.R.; Saha, B.C. and Malik, F.B. Phys. Lett. A 2006, **354**, 449.
28. Haque, A.K. F.; Uddin, M.A.; Basak, A.K.; Karim, K.R.; Saha B.C. and Malik, F.B. Phys. Rev. A 2006, **73**, 052703.
29. Haque, A.K. F.; Uddin, M.A.; Basak, A.K.; Karim, K.R.; Saha, B.C. and Malik, F.B. Physica Scripta **74**, 377 (2006).
30. Fontes, C.J.; Sampson, D.H.; Zhang, H.L. Phys. Rev. A 1999, **59**, 1329.
31. Desclaux, J.P. At. Data Nucl. Data Tables 1973, **12**, 325.
32. Amusia, M.Y.; Chernysheva, L.V. Computations of Atomic Processes, Institute of Physics Publishing, Bristol, 1997.
33. Shah, M.B.; Elliott, D.S.; Gilbody, H.B. J. Phys. B 1987, **20**, 3501.
34. Kuo, T.Y.; Chen, C.J.; Hsu, S.W.; Huang, K.N. Phys. Rev. A 1993, **48**, 4646.
35. Uddin, M.A., Haque, A.K.F.; Basak, A.K.; Saha, B.C. Phys. Rev. A 2004, **70**, 032706.
36. Peart, B.; Dolder, K.T. J. Phys. B 1969, **2**, 1169.
37. Tinschert, K.; Müller, A.; Hoffmann, G.; Hubert, K.; Becker, R.; Gregory, D.C.; Salzborn, E. J. Phys. B 1989, **22**, 531.
38. Fontes, C.J.; Sampson, D.H.; Zhang, H.L. Phys. Rev. A 1993, **48**, 1975.
39. Younger, S.M. Phys. Rev. A 1980, **22**, 111.
40. Aichele, K.; Hertenfeller, U. J. Phys. B 1998, **31**, 2369.
41. Donets, E.D.; Ovsyannikov, V.P. Sov. Phys. JETP 1981, **53**, 466.
42. Kunc, J.A. J. Phys. B 1980, **13**, 587.
43. Shi, X.H.; Chen, C.Y.; Zhao, Y.; Wang, Y.S. J. Quant. Spectrosc. Radiat. Transfer 2005, **91**, 161.
44. Marrs, R.E.; Elliott, S.R.; Scofield, J.H. Phys. Rev. Lett. 1994, **72**, 4082.
45. O'Rourke, B.; Currell, F.J.; Kuramoto, H.; Li, Y.M.; Ohtani, S.; Tong, X.M. et al., J. Phys. B 2002, **34**, 4003.
46. Watanabe, H.; Currell, F.J.; Kuramoto, H.; Ohtani, S.; O'Rourke, B.; Tong, X.M. J. Phys. B 2002, **35**, 5095.
47. Moores, D.L.; Reed, K.J. Phys. Rev. A 1995, **51**, R9.
48. Marrs, R.E.; Elliott, S.R.; Knapp, D.A. Phys. Rev. Lett. 1994, **72**, 4082.

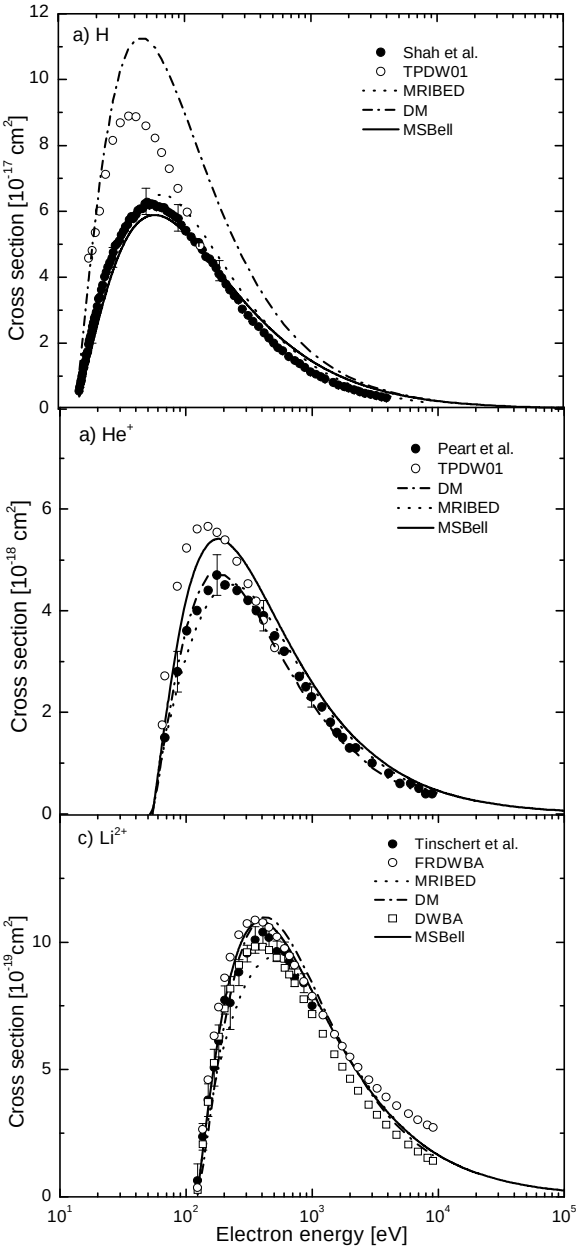

Fig.1. Electron impact ionization cross sections of *H*-like targets: a) H, b) He^{1+}, and c) Li^{2+}.

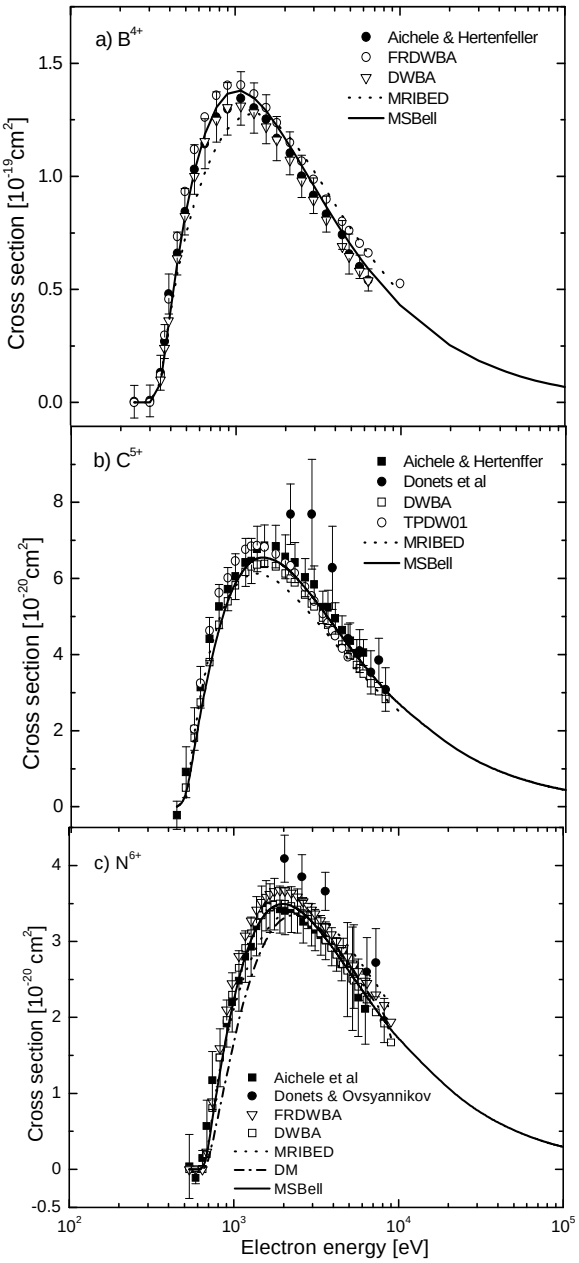

Fig.2. Same as in figure 1 for: a) $B^{4+,}$
b) C^{5+}, and c) N^{6+}.

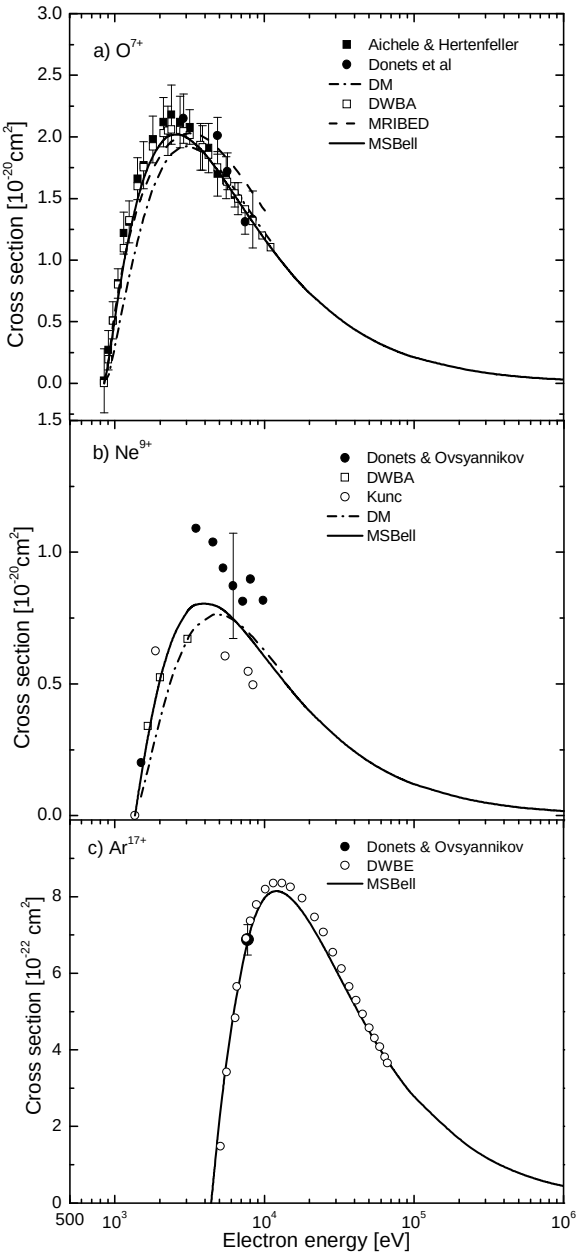

Fig.3. Same as in figure 1 for: a) O^{7+}, b) Ne^{9+}, and c) Ar^{17+}.

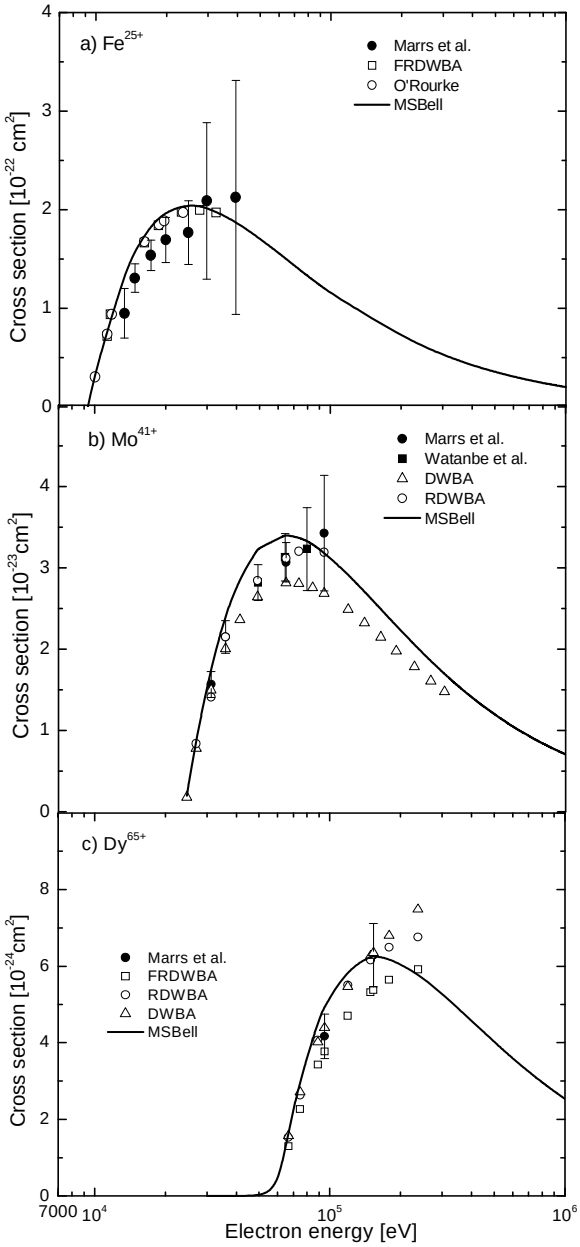

Fig.4. Same as in figure 1 for: a) Fe^{25+}, b) Mo^{41+}, and c) Dy^{65+}.

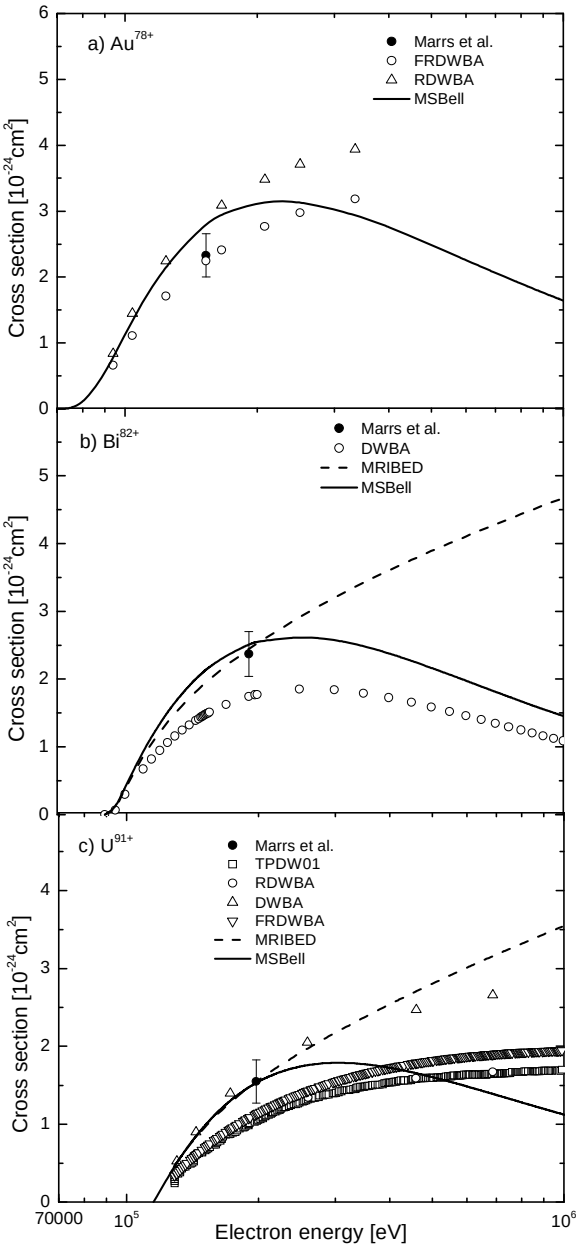

Fig.5. Same as in figure 1 for: a) Au^{78+},
b) Bi^{82+}, and c) U^{91+}.